Electronic supplementary information

Multi-site occupancy high-efficient $CaY_2ScZrAl_3O_{12}:Cr^{3+}$, Ce^{3+} phosphor for application in broadband NIR pc-LEDs

*Xiaole Xing, Xiaobin Wei, Yining Wang, Lingkang Yu and Mengmeng Shang**

Experimental section

1 Materials and synthesis

The sample denoted as CYSZA, comprising xCr^{3+} and yCe^{3+} ($0.02 \leq x \leq 0.22$, $0 \leq y \leq 0.07$), was synthesized using the high-temperature solid-state reaction method. The constituent raw materials, encompassing $CaCO_3$ (Sinopharm Chemical Reagent Co, 99.99%), Y_2O_3 (Jining Tianyi New Materials Co., Ltd, 99.99%), Sc_2O_3 (Jining Tianyi New Materials Co., Ltd, 99.99%), ZrO_2 (Jining Tianyi New Materials Co., Ltd, 99.5%), Al_2O_3 (Sinopharm Chemical Reagent Co, 99.99%), Cr_2O_3 (Aladdin, 99.95%), and $Ce_2(CO_3)_3$ (Sinopharm Chemical Reagent Co, 99.99%), underwent meticulous weighing and grinding in an agate mortar for a duration of 30 minutes to attain uniformity. To optimize reaction kinetics and ensure thorough synthesis, a precisely measured 2 wt% of CaF_2 (Aladdin, 99.5%) was strategically incorporated as a flux under precisely controlled stoichiometric conditions. Following the synthesis process, the resultant powder was subjected to a preliminary pre-sintering stage at 600°C for a duration of 4 hours, succeeded by a main sintering step at 1600°C for an additional 4 hours under a reducing ($N_2 : H_2 = 9 : 1$) atmosphere provided by a tube furnace. Post-sintering, the synthesized phosphor was gradually cooled to ambient temperature and meticulously pulverized into a fine powder, primed for subsequent experimental analyses.

2 Characterization

Powder X-ray diffraction (XRD) analyses were conducted utilizing a D8 Focus diffractometer (Bruker) employing Cu-Kα radiation (λ = 0.15405 nm) to scrutinize the material's composition and

phase. The acquired XRD data were refined using the General Structure Analysis System (GSAS) software suite, ensuring precise characterization and thorough examination of the sample. Field emission scanning electron microscopy (FE-SEM) coupled with energy dispersive spectroscopy (EDS) was utilized, employing the S4800 model from Hitachi. This integrated approach allowed for comprehensive examination and characterization of the sample's structural features and elemental constituents. Photoluminescence (PL) spectra, photoluminescence excitation (PLE) spectra, lifetime curves, time-resolved spectra (TRES), and temperature-dependent PL spectra were obtained using an Edinburgh fluorescence spectrometer (FLS980), which covers a temperature range from 100 to 475 K. The equipment is equipped with a 450 W continuous xenon lamp for steady-state excitation, a high-energy pulsed xenon lamp (uF2) for transient excitation, and a temperature control stage (TAP-02) for precise temperature control, enabling comprehensive analysis under controlled experimental conditions. The acquisition of diffuse reflectance (DR) spectra was performed using an ultraviolet-visible-NIR spectrophotometer (UV-3600 plus, Shimadzu, Japan). The quantum yield of the sample was measured using the absolute photoluminescence quantum efficiency measurement system C9920-02 (Hamamatsu Photonics, Japan). Evaluation of electroluminescence performance was conducted using the HAAS 2000 photoelectric measurement system from EVER FINE.

Table S1. Main parameters of processing and refinement results of CYSZA.

Compound	CYSZA
Space group	Ia-3d
a (Å) = b (Å) = c (Å)	12.377
V (Å^3)	1896.165
α (°) = β (°) = γ(°)	90
R_{wp}, %	12.7
R_p, %	8.34

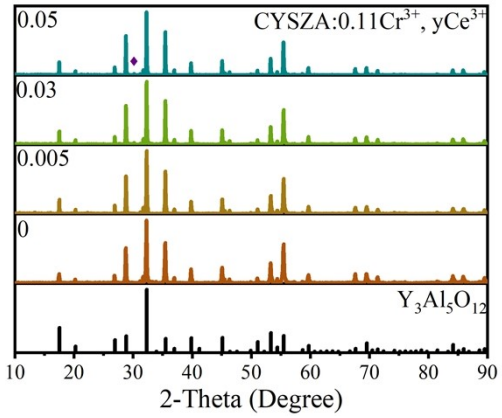

Fig. S1. The XRD patterns of CYSZA:0.11Cr^{3+}, yCe^{3+} compared with the standard card of YAG (PDF-75-1853).

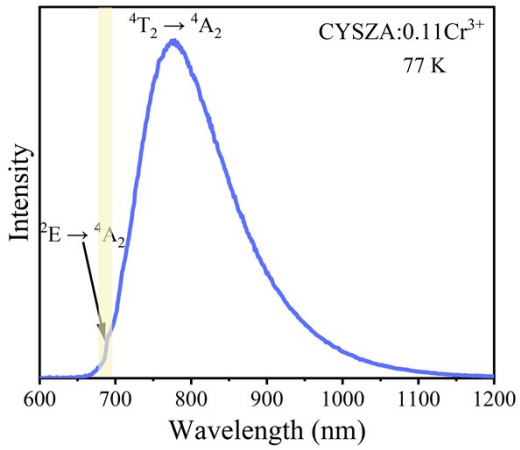

Fig. S2. PL spectra of CYSZA:0.11Cr^{3+} at 77 K.

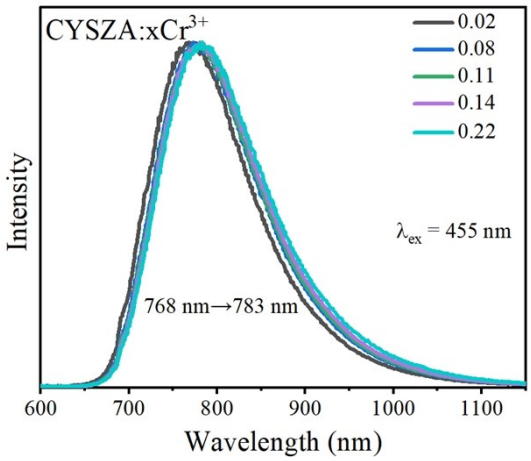

Fig. S3. Normalized PL spectra of CYSZA:xCr^{3+}.

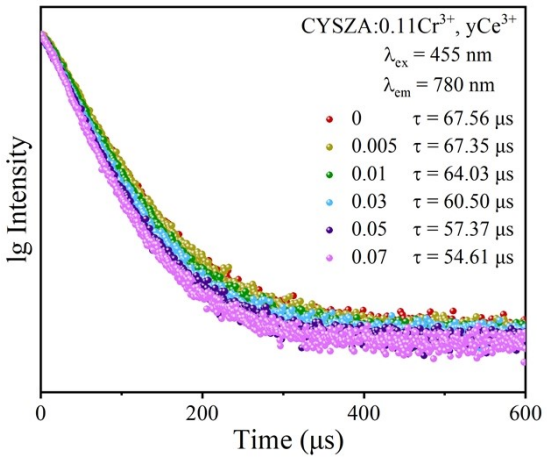

Fig. S4. Fluorescence decay curves of representative CYSZA:0.11Cr^{3+}, yCe^{3+} samples monitored at 780 nm.

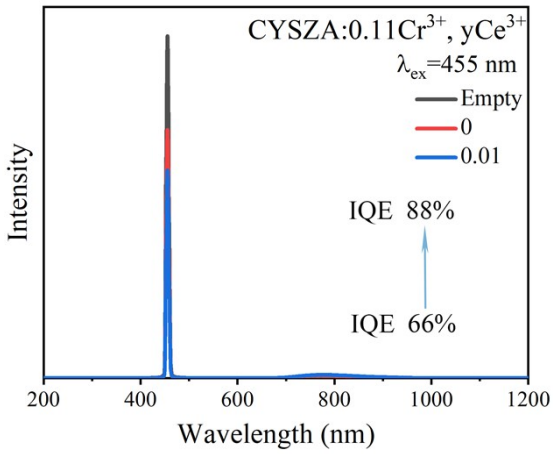

Fig. S5. Internal quantum efficiency (IQE) of CYSZA:0.11Cr^{3+} and CYSZA:0.11Cr^{3+}, 0.01Ce^{3+}.

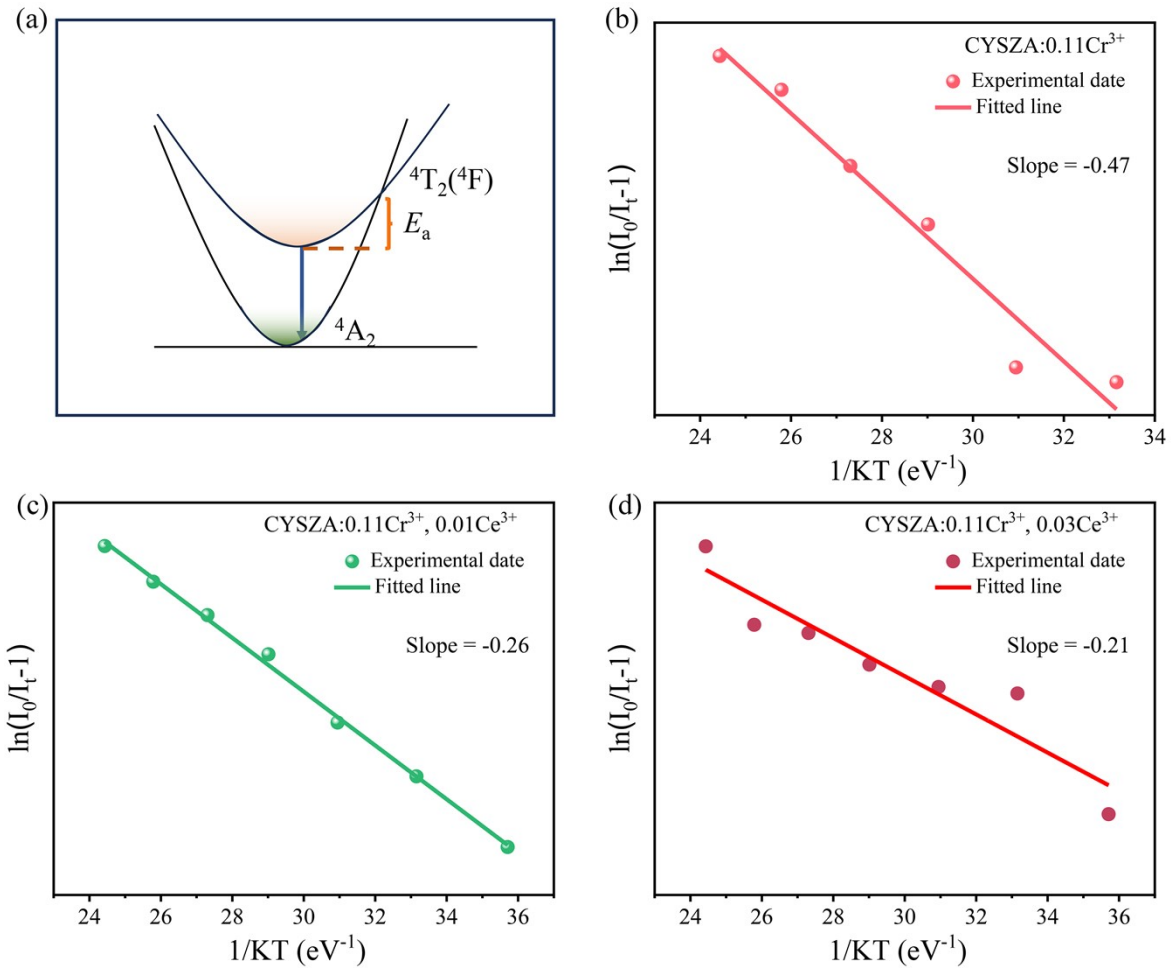

Fig. S6. (a) Configurational coordinate diagram illustrating thermal quenching behaviors. The Arrhenius fitting for (b) CYSZA:0.11Cr^{3+}, (c) CYSZA:0.11Cr^{3+}, 0.01Ce^{3+} and (d) CYSZA:0.11Cr^{3+}, 0.03Ce^{3+}.